Life prediction of RC bridge slabs under cyclic moving load

Hokkaido University　Student member　○Pengru DENG
Hokkaido University　Member　Takashi MATSUMOTO

1. INTRODUCTION

Around the world, a slab-on-girder superstructure is one of the most common structural systems used for highway bridges. In this system, the deck slab is one of the bridge elements most susceptible to fatigue failure. However, the employed theories for design of RC slabs focused on a flexural capacity regardless of a shear capacity of RC slabs. A brittle and catastrophic punching shear failure mode has been reported in North American, Europe, Japan, etc.

As the observed shortened fatigue life and punching shear failure mode of RC slabs in service was successfully reproduced under cyclic moving loads in [1], a moving load set-up was widely employed in experiments. According to the failure crack pattern of slabs under cyclic moving loads, an empirical life prediction equation was formulated as a function of a punching shear capacity of an assumed beam in [1] through fitting experimental data statistically. Employing finite element method, the punching shear failure mode was reproduced through finite element analysis of RC slabs in [2] as well. However, due to the widely-spread cracked element before failure, all the FEM trials were very time-consuming. Obviously, existing researches possess their own disadvantages. For the empirical life prediction equations, since the equations were from statistically fitting experimental data, the inner degradation mechanisms cannot be reflected. In terms of the numerical approaches, convergence problems were commonly encountered before failure. In addition, the numerical analyses are very time-consuming. Therefore, innovation of an efficient and sophisticated life prediction method considering the dominant degradation mechanisms of RC bridge slabs under cyclic moving loads should be meaningful for structural design, maintenance and strengthening. This is what was attempted in this study.

In this study, a theoretical fatigue life prediction method is proposed focusing on the propagation of punching shear cracks of a critical RC beam simplified from an RC slab under cyclic moving loads according to the degradation process and failure crack pattern. Fatigue crack growth is assumed as a result of concrete bridging degradation and rebar/concrete interface bond-slip degradation. Referencing to the failure model and employing the obtained fatigue crack growth, the fatigue life is predicted based on certain punching shear capacities combined with experimental observations. The applicability and reliability of the resulting method are confirmed with encouraging results from a comparison with experimental results and existing empirical equations. In addition, this method can not only accounting for the degradation mechanisms but also very time-saving (1-2 hours/load which is only a small percentage of that for numerical methods), which make it extremely suitable for parametric study and further design code improvement.

2. PROBLEM SIMPLIFICATION

For an RC slab under cyclic moving loads, a typical failure crack pattern is shown as Fig. 1 and the cracking process can be explained as follows: (1) Due to the existence of supporting girders, a drying shrinkage of concrete is constrained and consequently micro shrinkage cracks initiate along the direction vertical to the moving load direction. Meanwhile, the moving load leads to the initiation of cracks along the same direction with the shrinkage cracks because of a smaller reinforcement ratio along the bridge axis direction for RC bridge slabs; (2) A bidirectional anisotropy characteristic of the RC slab increases with the increasing number of cracks vertical to the moving load direction and propagations of the initiated cracks in (1). These parallel cracks, which can be observed from b-b cross-section in Fig. 1, divide the RC slab into several RC beams. An RC beam at mid-span is a critical beam. The width of the beam can be determined following [1]; (3) Due to an isolating effect of the parallel cracks, shear forces cannot be transferred effectively to the adjacent RC beams when the moving load moves onto one RC beam and also the critical beam; (4) In the critical beam, a large shear stress is concentrated around the loading area. It is this shear stress that leads to propagation of a couple of punching shear cracks symmetrical with respect to the moving load and the final brittle punching shear failure.

According to the cracking process and failure crack pattern of RC slabs under cyclic moving loads, an empirical life prediction equation was formulated [1], where the punching shear capacity of a critical RC beam is the only parameter used, which indicates that the fatigue life of the RC slab depends on the fatigue life of the critical RC beam. Geometries of this criterial RC beam is shown in Fig. 2, where h and l are the depth and span of the RC beam, respectively; l_w and b are the length and width of the wheel/beam contact area; d_e is the effective depth for tensile rebar.

Therefore, according to the theories of existing researches and the fatigue behavior of RC slabs under cyclic moving loads, the life prediction of an RC bridge slabs under a cyclic moving load can be simplified into the life prediction of a critical RC beam focusing on the propagation of punching shear cracks which are assumed to propagate along 45° lines symmetrical with respect to the moving load as shown in Fig. 2.

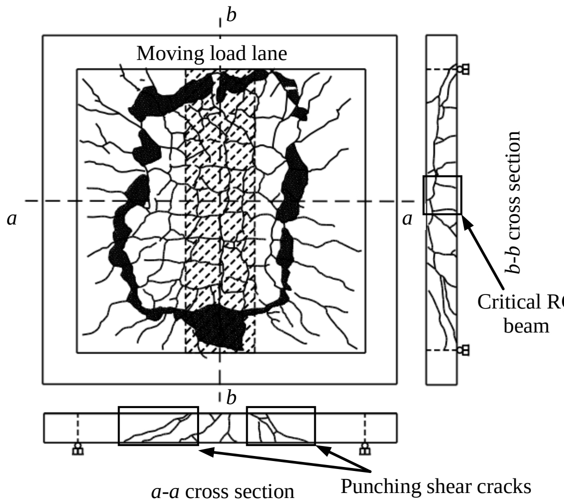

Fig. 1 A typical failure crack pattern of an RC slab under cyclic moving loads

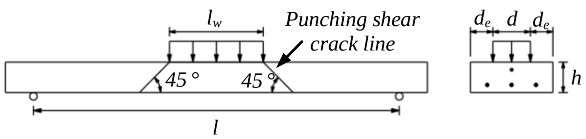

Fig. 2 Geometry of the simplified RC beam and the punching shear cracks

3. BASIC ASSUMPTION

For the critical RC beam subjected to general loads, sectional stresses which are obtained through cutting the beam vertically from the tip of the punching shear cracks are shown in Fig. 3. In this study, to determine all the sectional forces and stresses appeared in Fig. 3, three widely accepted assumptions are employed as follows:

(1) Plane cross-section assumption: From this assumption, the strain distribution (ε_{II}) at the uncracked concrete and the normal strain of rebar on both compression (ε_{ru}) and tension zone (ε_{rb}) can be related to α and β as

$$\varepsilon_{II}(x)=\varepsilon_t\left(1-\frac{x-\alpha h}{\beta h-\alpha h}\right) \tag{1}$$

$$\varepsilon_{ru}=-\varepsilon_t\frac{h-(c+d_b/2)-\alpha h}{(\beta-\alpha)h} \tag{2}$$

$$\varepsilon_{rb}=\varepsilon_t\frac{h-(c+d_b/2)}{(\beta-\alpha)h} \tag{3}$$

where c and d_b are the cover depth and rebar diameter, respectively. With these strains, the stress distribution of uncracked concrete (σ_{II}) and rebar normal forces (T_{rb} and T_{ub}) can be determined if the stress-strain relations for uncracked concrete and rebars are available.

(2) The cracked cross-section is assumed to rotate around the neutral axis. From this assumption, the normal strain (ε_{rb}) and shear strain (γ_{rb}) for the longitudinal rebars in the beam can be related as:

$$\gamma_{rb}=\varepsilon_{rb}\cdot\tan\varphi \tag{4}$$

where φ is as shown in Fig. 3. Taking into account the relation between shear elastic modulus and normal elastic modulus and assuming the Poisson's ratio (v) for steel is 0.3, we can obtain

$$V_{rb}=0.4T_{rb}\tan\varphi \tag{5}$$

This shear force is the well-known dowel effect of rebars.

(3) The crack has a linear crack opening profile. From this assumption, the crack width ($w(x)$) at any location (x) along the crack can be expressed by the crack mouth opening displacement (CMOD, δ) and crack depth ratio (α) as

$$w(x)=\delta\left(1-\frac{x}{\alpha h}\right) \tag{6}$$

Therefore, the concrete bridging stress distribution σ_I can be expressed by δ following a concrete bridging model.

In summary, except for the shear stress of uncracked concrete, all the reaction stresses of concrete and rebars can be expressed with three cracking state parameters, i.e. α, β and δ, based on the assumptions combining material models. To get α, β and δ after every loading cycle, at least three independent equations with unknown of α, β and δ should be established.

4. PROBLEM FORMULATION

4.1 Governing equation with *α*, *β* and *δ*

Referencing to the Fig. 3, there are two force equilibrium equations along x and y directions and one moment equilibrium equation, can be established. However, the force equilibrium equation along y axis is not available because the shear stress distribution for a cracked cross section is not fully cognized so far. The remaining two available equations are given as:

$$\int_0^{\alpha h}\sigma_I(x)dx+\int_{\alpha h}^{h}\sigma_{II}(x)dx+T_{rb}+T_{ru}=0 \tag{7}$$

$$\int_0^{\alpha h}\sigma_I(x)[(h-x)+(\alpha h-x)]dx+\int_{\alpha h}^{h}\sigma_{II}(x)(h-x)dx + T_{rb}\cdot(h-a_s)+V_{rb}\cdot(\alpha h-a_s)+T_{ru}\cdot a_s=M_A \tag{8}$$

where M_A is sectional moment due to applied loads.

In order to obtain a complete solution, another relationship is necessary. According to the cracking analysis of RC structures in [3], a CMOD decomposition equation can be established following, which is formulaically expressed as

$$\delta=\delta_A(\alpha)+\delta_I(\sigma_I(x),\alpha)+\delta_{rb}(T_{rb},V_{rb},\alpha)+\delta_s(T_{rb}) \tag{9}$$

where δ_A is CMOD due to applied load. δ_I are δ_{rb} are CMODs due to concrete bridging stress and rebar bridging forces, respectively. With crack face acting stresses due to applied loads, concrete and rebar bridging stresses, these three CMODs can be calculated employing a fracture mechanics based integral equation introduced in [3] if crack face weight functions for the crack geometry are available. For shear cracks in RC beam, the crack face weight functions are obtainable based on a finite element method (FEM) based virtual crack extension technique as shown in [4]. δ_s is CMOD due to bond slip which can be determined following an appropriate bond slip model.

Therefore, if all stresses and forces appeared in Eq. (7) to Eq. (9) can be expressed with α, β and δ, the cracking state parameters after every loading cycle are obtainable through solving Eq. (7) to Eq. (9).

4.2 Formulate sectional stresses and forces with *α*, *β* and *δ*

(1) Sectional forces and stresses due to applied loads: According to the transferring characteristic of moment and shearing force, sectional moment (M_A) and shearing force in the critical RC beam can be obtained from finite element analyis of the RC slab and analysis of the RC beam, respectively. With the obtained sectional moment and shearing force, stresses that would exist along the punching shear crack line in the absence of the crack can be easily expressed with α, β and δ from sectional analysis.

(2) Stresses from uncracked concrete can be expressed with α, β and δ through multiplying the concrete strain from Eq. (1) and elastic modulus of concrete. No degradation is assumed for uncracked concrete.

(3) Stresses from cracked concrete: In the first cycle, stresses from cracked concrete is expressed with α, β and δ following an empirical concrete bridging model [5] and using the crack opening displacement profile from Eq. (6). Under repetitive crack opening and closing process, there should be some degradations of concrete bridging stress. From 2nd loading cycle to the final failure, this degradation is accounted for based on a concrete bridging degradation model.

(4) Rebar stresses: In cracked RC structures, due to a rebar/concrete interface bond related tension stiffening effect, the stress-strain relation for rebars embedded in concrete should be different from that of bare bars. Thus, in this study, firstly the rebar stress-strain relation is modified incorporating multi-crack effect and bond-slip effect. And then, the rebar stresses are obtained through substituting rebar strain in Eq. (3) into this modified rebar stress-strain relation. From 2nd loading cycle to the final failure, the rebar stresses variation due to bond slip degradation is considered through introducing a bond slip degradation model.

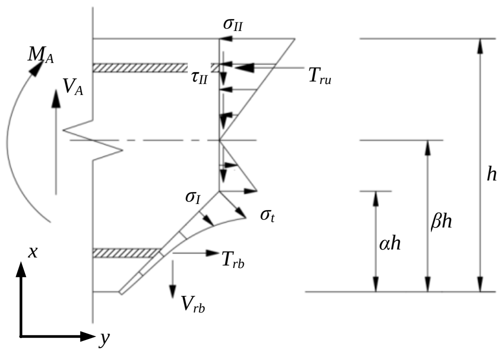

Fig. 3 Sectional stresses and forces

4.3 Failure moment determination *α*, *β* and *δ*

In this study, using the obtained cracking state parameters after every loading cycle, the final failure moment of RC slabs under cyclic moving loads is determined following some shear capacity based failure criterion.

As is generally accepted, the total shear resistance for a traditional RC slab is given by

$$V_R = V_c + V_{dow} \tag{10}$$

where V_c is the vertical component of the shear strength of concrete, V_{dow} is the dowel action of flexural reinforcement.

Under cyclic moving loads, the formed cracks experience repeated opening and closing process, which keeps polishing the interface of aggregates and mortar. As a result, only uncracked concrete can provide shear resistance. Therefore, in this study, V_c is obtained by integrating the vertical components of the tensile stresses in uncracked concrete following the AASHTO and ACI equations for punching shear. The equation for concrete punching shear capacity can be expressed as

$$V_c = 2[b + (1-\alpha)h]\cdot(1-\alpha)h\cdot f_t \tag{11}$$

In terms of the ultimate dowel force, an equation in [1] is employed in determining the ultimate dowel force of both tensile and compressive rebars as

$$V_{dow} = 2c\cdot B\cdot f_t \tag{12}$$

Substituting Eq. (11) and Eq. (12) into Eq. (10), the punching shear capacity of an RC beam simplified from an RC slab under cyclic moving loads is related to the cracking state parameters as

$$V_R = 2[b + (1-\alpha)h]\cdot(1-\alpha)h\cdot f_t + 4c\cdot B\cdot f_t \tag{13}$$

However, post-moment inspections of tested specimens showed that a delamination at the upper rebars level occurred in the mid-span cross-section of specimens subjected to cyclic moving loads. This is probably a result of high-fatigue shear stresses at that depth due to the existence of upper rebars and a short distance from the neutral axis. Therefore, the dowel effect of upper rebars should not be included in determining the punching shear capacity after the crack tip reaches upper rebars.

In summary, the punching shear capacity of a critical RC beam is given as

$$V_{pun} = \begin{cases} 2[b + (1-\alpha)h]\cdot(1-\alpha)h\cdot f_t + 4c\cdot B\cdot f_t \\ \qquad \text{Before crack tip reaching upper rebars} \\ 2[b + (1-\alpha)h]\cdot(1-\alpha)h\cdot f_t + 2c\cdot B\cdot f_t \\ \qquad \text{After crack tip reaching upper rebars} \end{cases} \tag{14}$$

The final failure moment is determined based on this punching shear capacity in this study.

5. NUMERICAL RESULTS AND EXPERIMENTAL VERIFICATION

In this study, a fatigue analysis based on the proposed method is conducted in order to investigate crack propagation and fatigue life of RC bridge slabs under cyclic moving loads. The method verification is done by comparing analysis results with results from experiments and some empirical equations. The fatigue analysis is conducted on an RC slab (C0) tested by Civil Engineering Research Institution for Cold Region (CERI) [6].

5.1 Prediction of fatigue crack growth

In this study, four load levels, i.e. 130 kN, 150 kN, 175 kN and 200 kN, are selected for fatigue analysis based on two considerations: (1) For loads lower than 130 kN, no solution can be obtained through solving Eq. (10) to Eq. (12), which means no crack initiates under these low loading levels; (2) As reported in [6], 200 kN is already about 70% of the static load capacity of the tested RC slab. Under a higher load level, before the formation of the parallel cracks observed in *b*-*b* cross section in Fig. 1, a punching shear failure may occur along both transverse and longitudinal directions similar to those under static load rather than along only transverse direction as under cyclic moving load. Under the selected loading levels, the crack depth/beam depth ratios are plotted with the number of loading cycles on the semi-logarithmic scale as shown in Fig. 4(a). Generally, the fatigue growth of a bridged crack in a concrete structure involves of three distinct stages: initial decelerated growth, steady state growth and final accelerated growth. Most of the fatigue life is spent in the second stage. It is found that the theoretical simulation successfully captured the first two stages, whereas the third stage cannot be observed in the curves. This can be explained as follows [7]. To facilitate understanding, a crack-tip stress intensity factor (SIF) which reflects the crack-tip stress state is employed for explanation. For the punching shear cracks, the net crack-tip SIF is a resultant of SIF from external applied load and all bridging effects. The SIF amplitude due to external applied load increases with the length of the crack emanating from the tension face. At the same time, the magnitude of the negative crack-tip SIF due to crack bridging (rebar forces and concrete bridging stresses) increases with the propagation of the crack as well. The initial decelerated growth is caused by the effective reduction of the net crack-tip stress intensity factor amplitude due to the rapidly increased crack bridging related SIF with the development of the crack length. The steady state growth is caused by the constant value of net crack-tip SIF when the increase of SIF due to applied load is balanced with the increase of negative SIF due to bridging stress. The reason why the final accelerated crack growth stage cannot be observed is that the RC beam is assumed to fail in a brittle shear failure mode according to certain failure criterion.

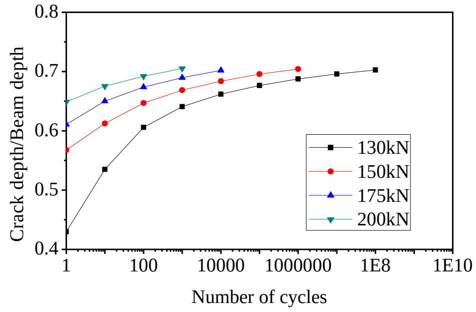

(*a*) *α* vs. number of loading cycles

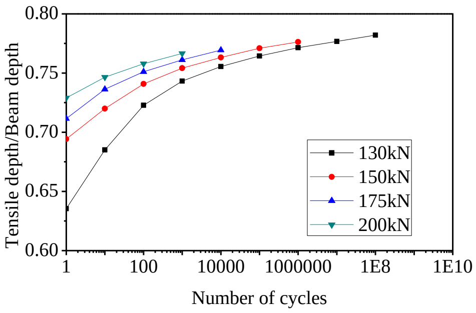

(*b*) *β* vs. number of loading cycles

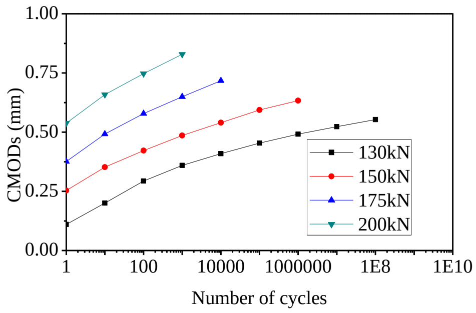

(*c*) *δ* vs. number of loading cycles

Fig. 4 Cracking state parameters vs. number of cycles

However, the initial decelerated stage in the crack depth/beam depth ratio to number of loading cycles curve for higher load level is not as apparent as that for lower load levels. This is because the punching shear crack is more fully developed in the beginning several loading cycles under the higher load levels, manifested with higher crack depths and wider crack openings. Due to the wide crack opening, the bridging effect from nonlinear concrete bridging stress maybe small or even negligible compared with that from rebars. Thus, the structure degradation can be regarded as mainly from the degradation of bond slip, which follows a steady state growth as shown in Fig. 4(a). As a result, the crack propagation curve seems to start from the steady state growth for higher load level as observed in Fig. 4(a).

Similar to the characteristics exhibited in the crack depth/beam depth ratio to the number of loading cycles relations, the two stages are also observed in Fig. 4(b), where the relationships between tensile depth/beam depth ratio and the number of loading cycles for several fatigue loading levels are plotted on the semi-logarithmic scale.

The evolution of CMODs with respect to the increasing number of loading cycles for several fatigue loading levels are drawn on a semi-logarithmic scale Fig. 4(c). It is noticed that the CMOD evolution of the punching shear crack depends on the load level. However, the two stages observed in Fig. 4(a-b) are not apparently exhibited. Especially for the second stage where a continuous increasing rather than a steady state of CMOD is observed for all load levels. As the crack depth reaches a stable state in the second stage, the CMOD due to applied load and crack bridging stress should stay almost unchanged. Thus, the CMOD increasing in the second stage is expected to be mainly from the degradation of bond slip.

5.2 Fatigue life prediction and comparison with existing methods and experimental results

In this method, the final fatigue failure of RC slabs under cyclic moving load is determined following certain brittle shear failure criterion introduced in section **4.3**. Substituting parameter values into Eq. (14), the punching shear load capacities for the moment of the crack tip reaching the upper rebars is determined as 230.63 kN. After the crack tip reaches the upper rebars, transverse shear cracks along the upper rebars initiate and propagate under repeated fatigue loads, which makes the dowel effect of upper rebars inefficient. These transverse shear cracks were observed in the mid-span cross section of the tested RC slab after failure in [6]. As a result, the punching shear capacity reduces to 123.79 kN. Therefore, under the selected cyclic moving loads, i.e. from 130 kN to 200 kN, fatigue punching shear failure occurs after the crack tip reaches the upper rebars, which is coincident to crack depth/beam depth ratio (α) equaling 0.7 for the employed case. Comparing this critical state with the obtained cracking state parameters vs. number of cycles curves shown in Fig. .4, the fatigue life of the RC slab subjected to different load levels can be determined easily.

Moreover, the fatigue life can be calculated following some empirical life prediction equations derived by different research groups, such as Matsui and Abe research teams, and institutions, such as JSCE and PWRI. Since these empirical equations were obtained through statistically fitting a huge amount of experimental data on RC slabs under cyclic moving loads, each empirical equation represents a set of experimental results of RC slabs which have different dimensions and were tested under different levels of cyclic moving loads. Thus, these equations implicitly reflect the internal mechanisms and can be employed in life prediction of similar problems as employed case in this study.

All the S-N diagrams from the proposed theoretical method and the empirical equations and experimental fatigue life are

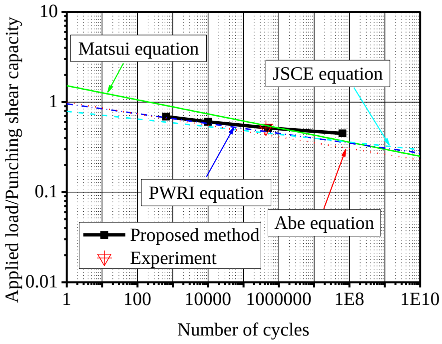

Fig. 5 Fatigue life from different approaches

plotted on a double-logarithmic scale as shown in Fig. 5 where the vertical and horizontal axes represent a load parameter normalized with a punching shear capacity determined by [1] and number of loading cycles, respectively. It is found that the theoretical S-N relation agrees well with the fatigue life of the experimental RC slab and is almost the average results of the four reported equations derived statistically. These good agreements verify the reliability of the proposed theoretical method.

6. CONCLUSIONS

A theoretical fatigue life prediction method for RC bridge slabs which fail in a punching shear model under cycle moving loads has been proposed in this study.

The method was established focusing on the propagation of punching shear cracks in a critical RC beam simplified from a RC slab under cyclic moving. Concrete bridging degradation and bond slip degradation were considered as the source of crack propagation. From this method, the fatigue crack growth were predicted, which were then employed in determining the failure moment based on some shear failure modes.

Comparisons between method predictions to results from experiment and some existing empirical life prediction equations indicate a good agreement, which confirmed the applicability and reliability of the proposed method.

REFERENCES

1) Maeda, Y. and Matsui, S.: Punching shear load equation of reinforced concrete slabs. Doboku Gakkai Ronbunshu, 133-141, 1984.
2) Drar, A. A. M. and Matsumoto, T.: Fatigue analysis of RC slabs reinforced with plain bars based on the bridging stress degradation concept. Journal of Advanced Concrete Technology, 14(1), 21-34, 2016.
3) Deng, P. and Matsumoto, T.: Estimation of the Rebar Force in RC Members from the Analysis of the Crack Mouth Opening Displacement Based on Fracture Mechanics. Journal of Advanced Concrete Technology, 15(2), 81-93, 2017.
4) Deng, P. and Matsumoto, T.:. Weight function determinations for shear cracks in reinforced concrete beams based on finite element method. Engineering Fracture Mechanics, 177, 61-78, 2017.
5) Stang, H., Li, V. C. & Krenchel, H.: Design and structural applications of stress-crack width relations in fibre reinforced concrete. Materials and structures, 28(4), 210-219, 1995.
6) Mitamura, H., Syakushiro, K., Matsumoto, T. and Matsui, S.: Experimental study on fatigue durability of RC deck slabs with overlay retrofit. Journal of Structural Engineering A, 58, 1166-1177, 2012.
7) Li, V. C. and Matsumoto, T.: Fatigue crack growth analysis of fiber reinforced concrete with effect of interfacial bond degradation. Cement and Concrete Composites, 20(5), 339-351, 1998.